Cell, Volume *138*

Supplemental Data

The F-BAR domain of srGAP2 induces membrane protrusions required for neuronal migration and morphogenesis

Sabrice Guerrier, Jaeda Coutinho-Budd, Takayuki Sassa, Aurélie Gresset, Nicole Vincent Jordan, Keng Chen, Wei-Lin Jin, Adam Frost, and Franck Polleux

Supplemental Experimental Procedures

Sequence Alignments

Sequence alignments for srGAPs were obtained using MUSCLE (Edgar, 2004). Human srGAP2 (gi|48427907|sp|O75044.2) Mouse srGAP2 (image:BC030547), Human srGAP1 (NP_065813.1), Mouse srGAP1 (NP_001074506.1), Human srGAP3 (NP_055665.1), Mouse srGAP3 (NP_536696.4), Xenopus srGAP (NP_001087899.1), C. elegans (NP_502179.1). Secondary structure was obtained for srGAP2 using hhpred (Soding et al., 2005) (http://toolkit.tuebingen.mpg.de/hhpred), Bioinfobank Metaserver (http://meta.bioinfo.pl) and PromaS3D (Pei et al., 2008) (http://prodata.swmed.edu/promals3d/promals3d.php). Structural alignments srGAP2 and F-BAR domains were obtained using hhpred (Soding et al., 2005), Bioinfobank Metaserver and PromalS3D (Pei et al., 2008). Mouse FBP17 (NP_062279.1), Mouse Syndapin1 (CAQ52060.1), Mouse FCHo2 (NP_766179.1), Mouse PSTPIP2 (CAJ18516.1), Mouse Fer (AAB18988.1).

shRNA design and validation

shRNA sequences were obtained from Dharmacon Dha2 Sense (5'- GAT CCA ATG GAC TAC TCT CGA AAC TTC AAG AGA GTT TCG AGA GTA GTC CAT TTC TTT TTT GGA AA-3') Dha2 Anti-sense (AGC TTT TCC AAA AAA GAA ATG GAC TAC TCT CGA AAC TCT CTT GAA GTT TCG AGA GTA GTC CAT TG) and Dha5 Sense (5'- GAT CCG CTA TCT GCT GAA TTA AAT CTT CAA GAG AGA TTT AAT TCA GCA GAT AGG ATT TTT TGG AAA-3') Dha5 Anti-sense (AGC TTT TCC AAA AAA TCC TAT CTG CTG AAT TAA ATC TCT CTT GAA GAT TTA ATT CAG CAG ATA GCG). These constructs were cloned into pSilencer 2.1 (ambion). These shRNA were subsequently cotransfected with srGAP2-EGFP into COS7 cells ((shRNA 1.5μg) and srGAP2-EGFP (.5μg)). Lysates were collected 48hrs. After transfection and level of knockdown was determined by western blot using rabbit anti-GFP (Molecular Probes).

Constructs

All constructs were cloned into pCIG2 vector (Hand et al., 2005), which contains a (cDNA)-IRES-EGFP under the control of a CMV-enhancer/chicken-β-actin promoter. srGAP2 (IMAGE clone# BC030457) was first mutagenized using Quickchange (Stratagene) to repair a point mutation at position 596 to avoid premature stop in transcription. srGAP2 was then subcloned into pEGFP-N1 (Clontech). The entire srGAP2-EGFP cassette was then subcloned into pCIG2 replacing the IRES-EGFP resulting in pCIG2::srGAP2-EGFP. srGAP2 was also cloned into pNeuroD-EGFP vector. All subsequent constructs were cloned similarly. F-BAR (aa1-501), srGAP2$^{\Delta F\text{-}BAR}$ (aa502-1045), srGAP2$^{\Delta FCH}$ (aa121-1045). srGAP2^{R527L}, srGAP2^{W765A}, srGAP2$^{\Delta Cterm}$, and srGAP2* (dha5 shRNA resistant, base pairs mutation T898C, A900G, and C904T) were generated by mutagenesis using Quickchange (Stratagene). F-BAR$^{\Delta 49}$ was generated by fusing amino acids (1-452) of human srGAP2 (accession number NM_015326) to the c-terminus of clone BC112927. This clone is a partial human duplication of the F-BAR of srGAP2 present in Chromosome 1p12 and encoding only the first nine exons (out of twenty-two in the original full length human srGAP2 (Sassa and Polleux, unpublished results). The first nine exons present in the 1p12 duplication encode for the F-BAR with the last 49 amino acids of the C-terminus are deleted, hence the name F-BAR$^{\Delta 49}$ due to a splicing defect (Sassa and Polleux, unpublished results). This splicing defect also results in the addition of seven additional amino acids to the deleted C-terminus that are not normally present in the F-BAR of srGAP2, as they arise from intronic sequence.

COS7 cell culture, transfections, staining and filopodia measurements

COS7 cells were cultured in DMEM + 10%FBS 2mM L-glutamine and penicillin/streptomycin. For transfections, cells were plated in 6 well dishes and lipofectamine 2000 (4μl) was mixed with 2μg of DNA in Opti-mem and added to cells for 3hrs. After 3hrs, serum-free media was replaces with DMEM + 10%FBS and cells were cultured for 24hrs. After 24hrs, cells were trypsanized and replated on poly-l-lysine coated coverslips and cultured for an additional 24hrs. Cells were then fixed using 4% paraformaldehyde. Cells were then washed 3 times in PBS, then blocked/permeablized in .3% triton-X 100 in PBS + 5% BSA (PBS-T) for 20 minutes. Cells were then incubated with alexa-546 phalloidin (1:200) in PBS-T overnight. Finally, cells were then washed 3 times in PBS-T and mounted.

To determine filopodia number, cells were imaged using LEICA TCS SL confocal microscope, 63x/1.4NA oil immersion objective. 2x zoomed images were taken of representative cells from each construct. Images were then imported to NIH ImageJ. Using the segmented line tool, a perimeter was drawn around the cells. The presence of filopodia was determined by counting the number of consecutive pixels on the line drawn around the cell perimeter and normalized by dividing the total number of filopodia by the cell perimeter (filopodia/microns).

For cytochalasin D treatments, COS7 cells were transfected with F-BAR-EGFP and cultured for 48hrs. Cells were then treated with 400μM cytochalasin D for 30 minutes. To observe the presence of F-actin, cells were fixed and stained with phalloidin. To observe dynamics, control, untreated cells were imaged for 10 minutes (picture taken every 10 seconds) and cytochalasin D treated cells were imaged for 27 minutes (picture taken every minute).

For transferrin uptake assay, COS7 cells were serum starved for one hour at 4 degrees in the presence of alexa-647 transferrin. Cells were then warmed to 37 degrees to allow uptake of transferrin and fixed and treated as described above.

Ex Vivo Cortical Electroporation and Primary Cultures

Mouse cortical progenitors were electroporated *ex vivo* at embryonic day (E) E15 as described (Hand et al., 2005). Briefly, cDNA constructs in overexpression experiments (1μg/μl) were injected into the lateral ventricle of each embryo and electroporated using an ECM 830 electroporator (BTX) with four 100 ms pulses separated by 100 ms intervals at 25V. Following electroporation, cerebral cortices were dissected and enzymatically dissociated as described previously (Polleux and Ghosh, 2002). $1.25x10^5$ cells were plated onto glass coverslips coated with poly-L-lysine and laminin and cultured in serum-free media (Basal Medium Eagle containing both B27 and N2 supplements, L-Glutamine and Penicillin/Streptomycin) and fixed in 4% paraformaldehyde for immunohistochemistry. For shRNA rescue experiments in dissociation a mixture (shRNA 1.5μg/μl) and srGAP2-EGFP* (0.5μg/μl) was injected into lateral ventricle. For slice cultures, embryonic brains were electroporated and dissected as described above. The brains were then embedded in 3% low temperature gelling agarose and 250 μm-thick vibratome sections were cut using a LEICA VT1000S vibratome and placed on poly-L-lysine/laminin coated transwell inserts and cultured organotypically using an air interface protocol (Polleux and Ghosh, 2002). shRNA expressing slices were cultured for 3 days in vitro and cDNA expressing sections were cultured for 5 days in vitro.

Time Lapse confocal microscopy of cortical sections

Using a Leica TCS-SL confocal microscope (mounted on a DM-IRE2 inverted microscope stand) and equipped with a X-Y motorized Märzhäuser stage, time-lapse confocal microscopy was performed by imaging multiple Z-stacks at pre-selected positions on a given set of electroporated slices as described previously (Hand et al, 2005). Slices were cultured on confocal inserts (Millipore, 5mm height) and imaged using a long distance 20x/0.4 NA objective. For shRNA expressing sections, pictures were taken at a frequency of 1 picture every 12 minutes for 4hrs. In the case of srGAP2 over-expression experiments, sections were imaged every 16 minutes for a maximum of 10hrs 24 minutes.

Dissociated cortical neuron culture

Cultured neurons and brain sections were stained as described previously (Ghosh and Polleux 2002). The following antibodies were used chicken anti-GFP (Upstate), mouse anti-Tuj1 (b-III tubulin) (Sigma), mouse anti-nestin (BD Bioscience), mouse anti-MAP2 (a/b isoforms; AP20 Sigma), rabbit anti-srGAP2 (gift of Gong Ju, Shanghai JiaoTong University; (Yao et al., 2008)), and F-actin was labeled using alexa-546 phalloidin (Sigma). All images were captured using a LEICA TCS SL confocal microscope. For staining of endogenous srGAP2 in acutely dissociated neurons, cells were fixed in 4% paraformaldehyde for 30 minutes. The cells were then washed with PBS three times. They were then permeabilized with .05% triton-x 100 for 20 minutes and washed again in PBS. They were then incubated in blocking buffer (5% bovine serum albumin (BSA) in PBS) for 30 minutes and incubated with srGAP2-A2 antibody (1:200 in .2% BSA in PBS) overnight. For F-actin staining, phalloidin was added at 1:200. Cells were subsequently washed in 0.2% BSA in PBS and the appropriate Alexa-conjugated secondary antibodies (Molecular Probes 1:2000) for 30 minutes. Cells were then washed in PBS and slides were mounted.

Quantification of neuron migration and neurite branching.

For shRNA treated slices, the extent of cell migration was analyzed as described previously (Hand et al., 2005). In cDNA expressing sections, migration was assayed to different ways: (1) high magnification pictures were taken of the cortical plate and IZ and we quantified the ratio of cells/μm^2 CP/ cells/μm^2 in the IZ; (2) For branching measurements, high magnification images were obtained of neurons migrating in layer 5/6 in various conditions. Number of branches protruding from the leading process were counted. For cell speed measurements in shRNA treated slices, nuclei position was tracked manually during each frame using NIH ImageJ. Cell speed was calculated using Microsoft Excel and speed was reported in micron/hr. Neurite branching was quantified using NIH ImageJ.

In situ hybridization

In situ hybridization was performed as previously described (Mattar et al., 2004).

Liposome Preparation

Folch Fraction I Brain Lipid Extract from bovine brain (B1502) in chloroform was obtained from Sigma-Aldrich (St. Louis, MO) and used without further purification. 10 mg of total lipid were added to a glass vial and dried at room temperature under streaming argon while vortexing in order to form a thin lipid film around the tube surface. The lipids were re-dissolved in absolute hexane, dried under argon again while vortexing, and then dessicated *in vacuo* for >2 hours to remove the last traces of chloroform. The dried lipid film was then pre-hydrated at RT with water-saturated N2 for 2 minutes

until the film became transparent. Buffer (50mM KCl/10mM/HEPES/1mM DTT, pH 7.4) was added to the hydrated lipid film to a final lipid concentration of 2 mg/ml. The vial was sealed under argon and incubated at RT for 2 h, and then gently rocked overnight to disperse the lipids into solution.

Electron Microscopy

Continuous carbon-coated Cu-grids were glow discharged in room air according to standard protocols. 4 μl of sample were added and allowed to sit for ~10 seconds before being blotted onto filter paper. The grid surface was then immediately stained with freshly prepared (<15 minutes) 0.8% uranyl formate. Images were acquired using a Philips Tecnai F12 microscope operating at 120 kV using nominal magnifications of 29-50,000x, and defocus values of –15,000 to –22,000 Å. Images were recorded on a Gatan 1K CCD. Image analysis, including tubule diameter measurements, were performed with NIH ImageJ.

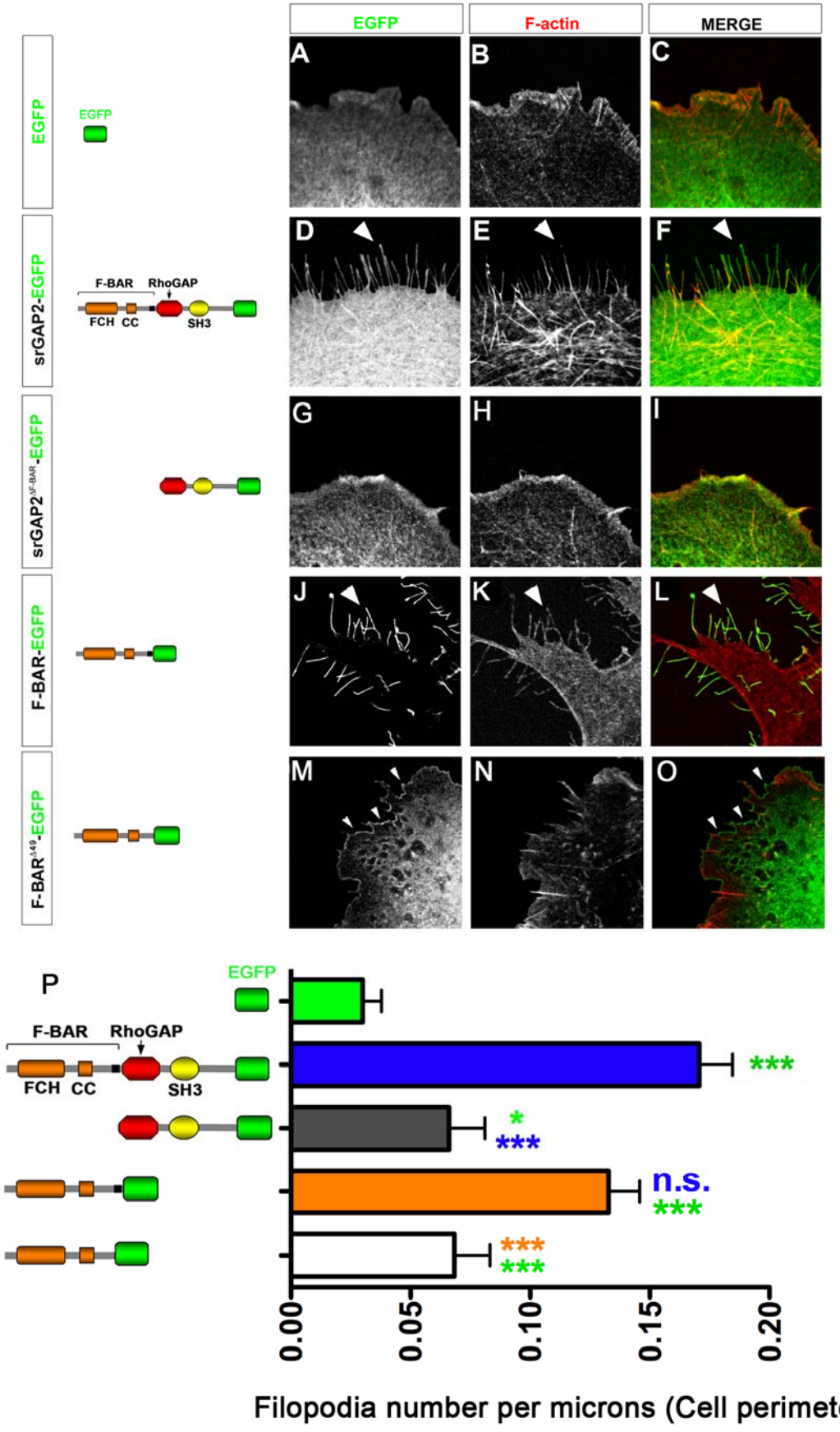
EGFP
F-actin
MERGE
EGFP
srGAP2-EGFP
srGAP2ΔF-BAR-EGFP
F-BAR-EGFP
F-BARΔ149-EGFP
F-BAR
RhoGAP
FCH
CC
SH3
A
B
C
D
E
F
G
H
I
J
K
L
M
N
O
P
EGFP
F-BAR
RhoGAP
FCH
CC
SH3
***
*
***
n.s.
***
***
***
0.00
0.05
0.10
0.15
0.20
Filopodia number per microns (Cell perimeter)

Figure S1. srGAP2 induces filopodia formation in a F-BAR-dependent manner in COS7 cells.

(A-C) COS7 cell expressing EGFP counter stained with phalloidin for F-actin (red).

(D-F) COS7 cell expressing srGAP2-EGFP fusion protein for F-actin-rich filopodia (arrowheads in D-F).

(G-I) Expression of srGAP2$^{\Delta\Delta F\text{-}BAR}$-EGFP fusion protein does not promote filopodia formation.

(J-L) Expression of the F-BAR-EGFP fusion protein is sufficient to promote filopodia formation in COS7 cells. Note the significant increase in membrane targeting to the extreme periphery of the cell (J-L) and induces the formation of long F-actin rich protrusions (J-L) like full-length srGAP2. Thus expression of the F-BAR domain of srGAP2 is sufficient to induce filopodia. Moreover this activity is not simply dependent on localization to the plasma membrane since expression F-BAR$^{\Delta 49}$-EGFP (M-O), which localized nicely to the plasma membrane, did not cause a significant increase in filopodia.

(P) Quantification of the effects described in A-O. (EGFP, n=41 cells; srGAP2-EGFP, n=52 cells; srGAP2$^{\Delta F\text{-}BAR}$-EGFP, n=21 cells; F-BAR-EGFP, n=21 cells; F-BAR$^{\Delta 49}$-EGFP, n= 15 cells. Cells were taken from 3 independent experiments and analyzed using Mann-Whitney Test * $p<0.05$, ** $p<0.01$, *** $p<0.001$. Green color indicates comparison to EGFP and blue color indicates comparison to srGAP2-EGFP and orange indicated comparison to F-BAR-EGFP).

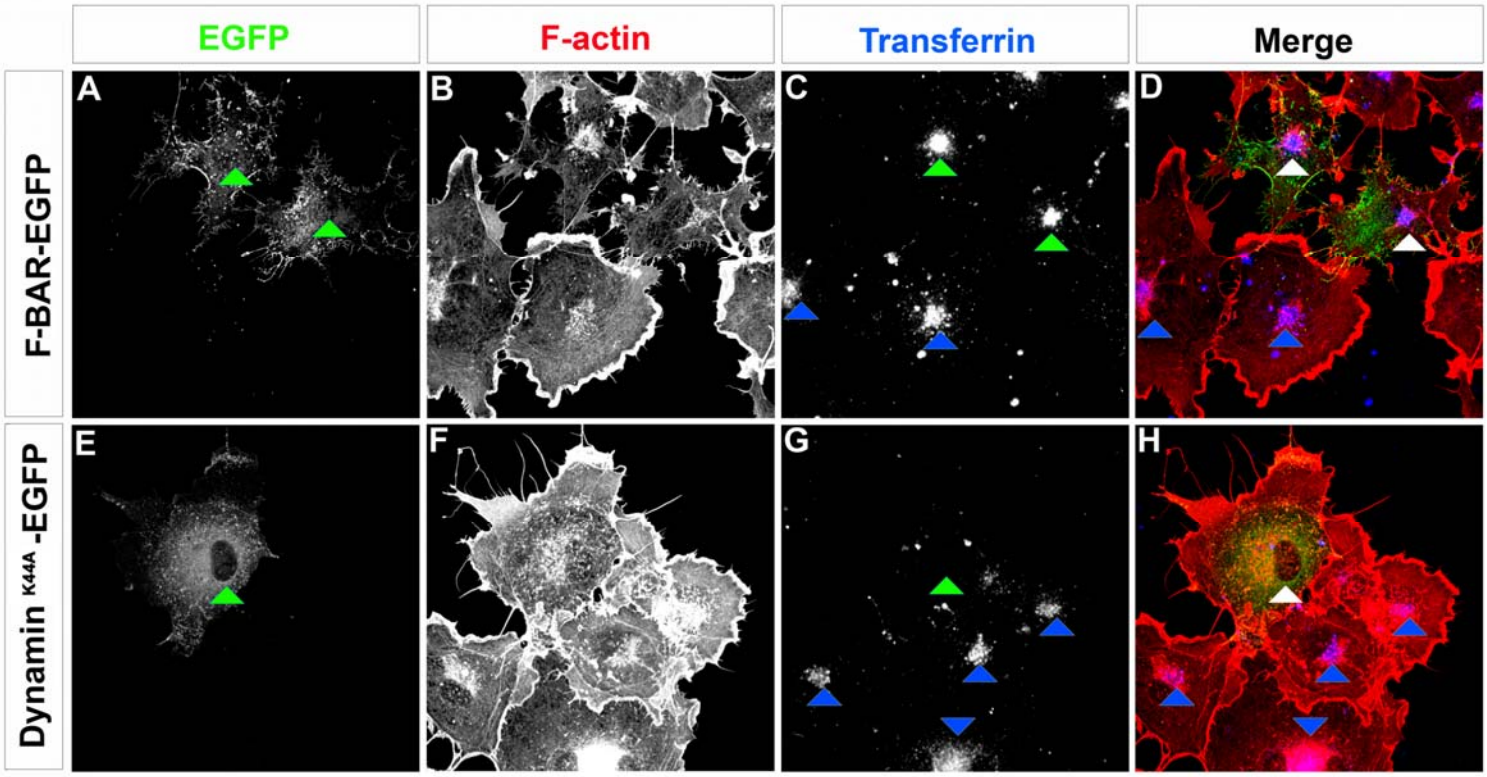

Figure S2. Expression of the F-BAR domain of srGAP2 in COS7 cells does not inhibit endocytosis.

(A-D) COS7 cells expressing the F-BAR-EGFP fusion protein were incubated with Alexa 647-conjugated transferrin then fixed and permeabilized and stained with Alexa546-phalloidin to label F-actin (B). This transferrin-uptake assay reveals no significant difference in the level of endocytosis between F-BAR-EGFP-expressing cells (white arrowheads in D) and untransfected cells (blue arrowheads in D).

(E-H) COS7 cells expressing Dynamin2^{K44A}-EGFP (dominant negative) were used as a positive control for inhibition of endocytosis as these cells were unable to endocytose transferrin (white arrowheads in H).

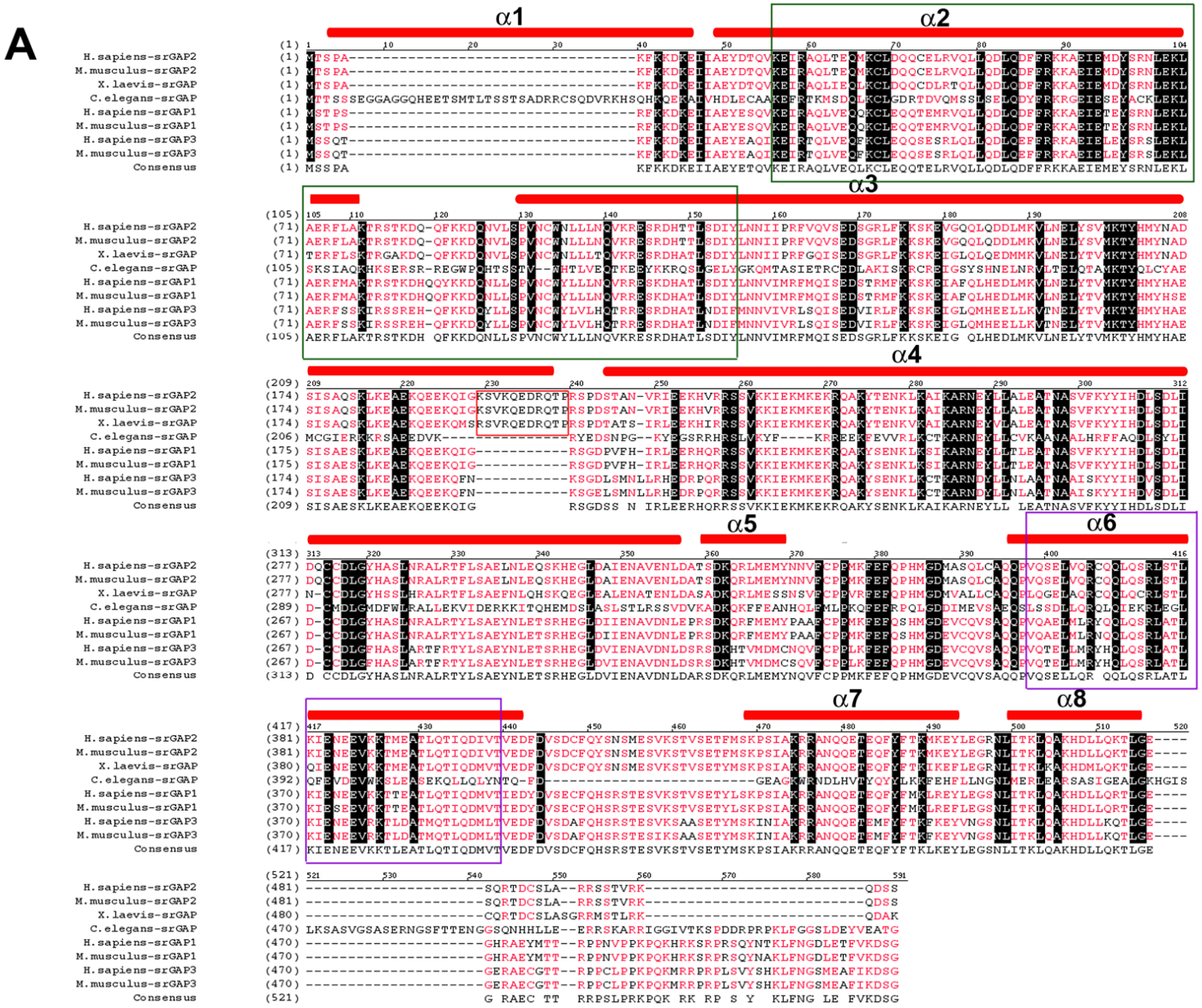
A
α1
α2
α3
α4
α5
α6
α7
α8
H.sapiens-srGAP2
M.musculus-srGAP2
X.laevis-srGAP
C.elegans-srGAP
H.sapiens-srGAP1
M.musculus-srGAP1
H.sapiens-srGAP3
M.musculus-srGAP3
Consensus

B

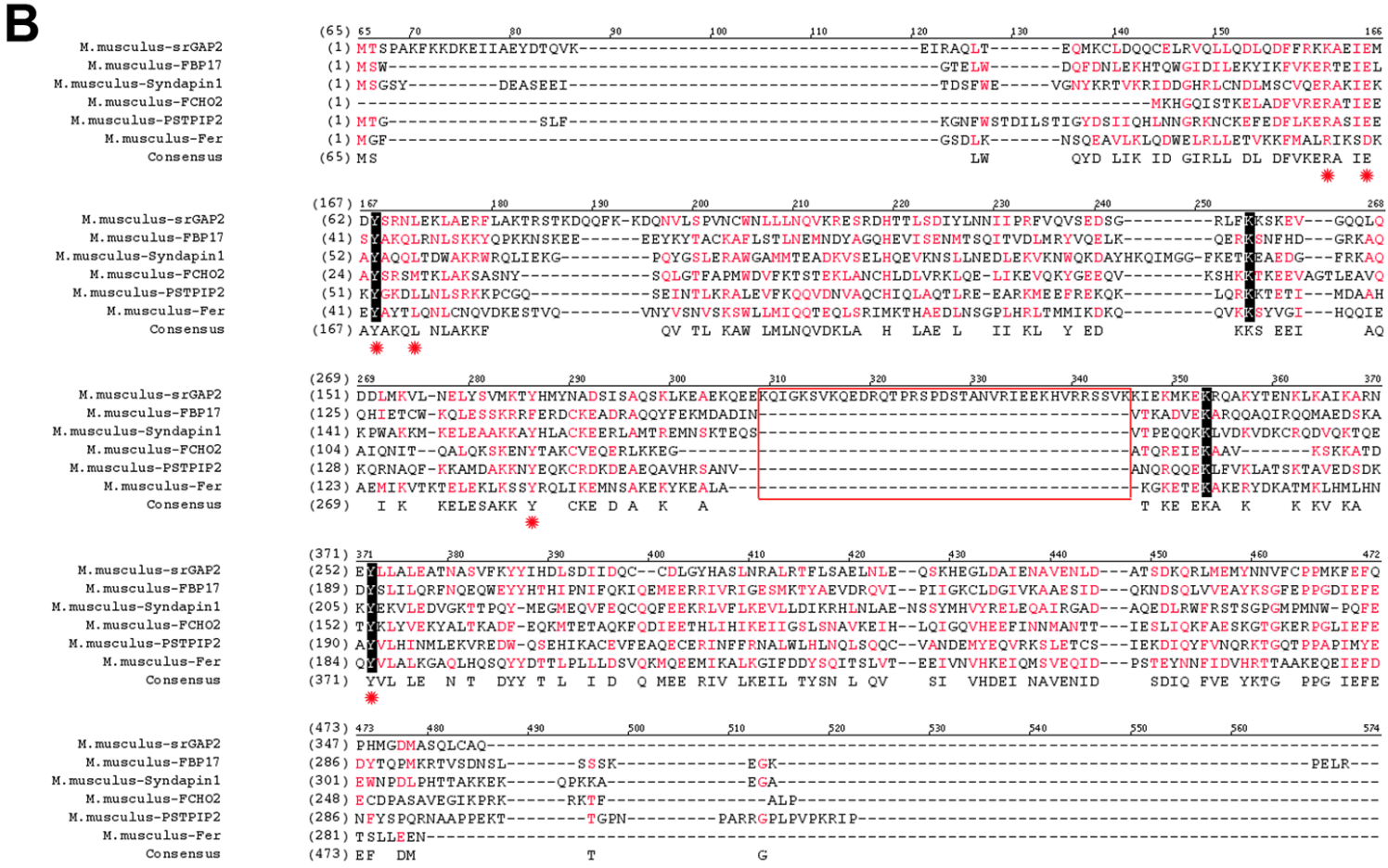
M.musculus-srGAP2
M.musculus-FBP17
M.musculus-Syndapin1
M.musculus-FCHO2
M.musculus-PSTPIP2
M.musculus-Fer
Consensus

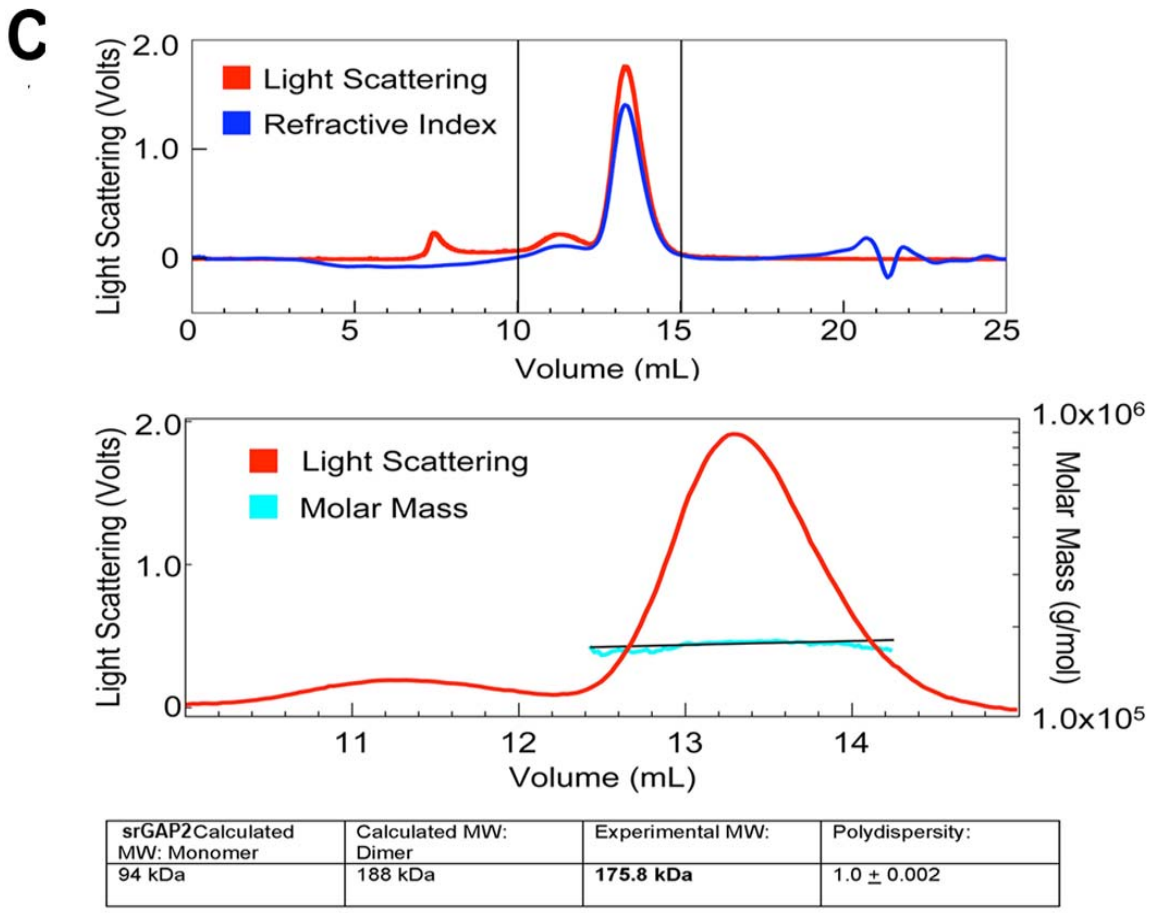

srGAP2Calculated MW: Monomer	Calculated MW: Dimer	Experimental MW:	Polydispersity:
94 kDa	188 kDa	**175.8 kDa**	1.0 ± 0.002

Figure S3. Structural alignment of the predicted F-BAR domain of srGAP2.

(A) Sequence alignment of the srGAP family of molecules from various species. Residues labeled in white on black background are identical. Red residues represent groups of conserved amino acids. srGAP2-specific insertion is boxed in red. Predicted alpha-helices are depicted as red bars (secondary structure prediction was obtained using hhpred (Soding et al., 2005) (http://toolkit.tuebingen.mpg.de/hhpred) and Bioinfobank metaserver (http://meta.bioinfo.pl). The F-BAR domain is defined by the alpha helices 2-4. However, three additional alpha-helices are predicted C-terminal of the 'minimal' F-BAR domain and precede the GAP domain.

(B) Structural alignment of mouse srGAP2 with representative mouse F-BAR domains was performed using PromalS3D (Pei et al., 2008) (http://prodata.swmed.edu/promals3d/promals3d.php) and hhpred. Residues colored white on black background are identical between sequences. Red residues represent conserved groups of amino acids. Red stars depict amino acids shown to reside at the dimer interface. Green boxes represent FCH domain as defined by SMART (http://smart.embl-heidelberg.de/). Purple boxes represent predicted coiled coil. Red box identifies srGAP specific insertion.

(C) Top panel: purified full-length srGAP2 protein (aa 1-786 containing F-BAR, GAP and SH3 domains) (300 μg) was loaded onto a Superose 6 column and separated by size exclusion chromatography. Lower panel: expanded view of the light scattering curve (red) in brackets, with the predicted molar mass depicted in cyan. The molecular weight of srGAP2 in solution was determined to be 175.8 kDa by fitting the molar mass curve to a linear function using Astra software.

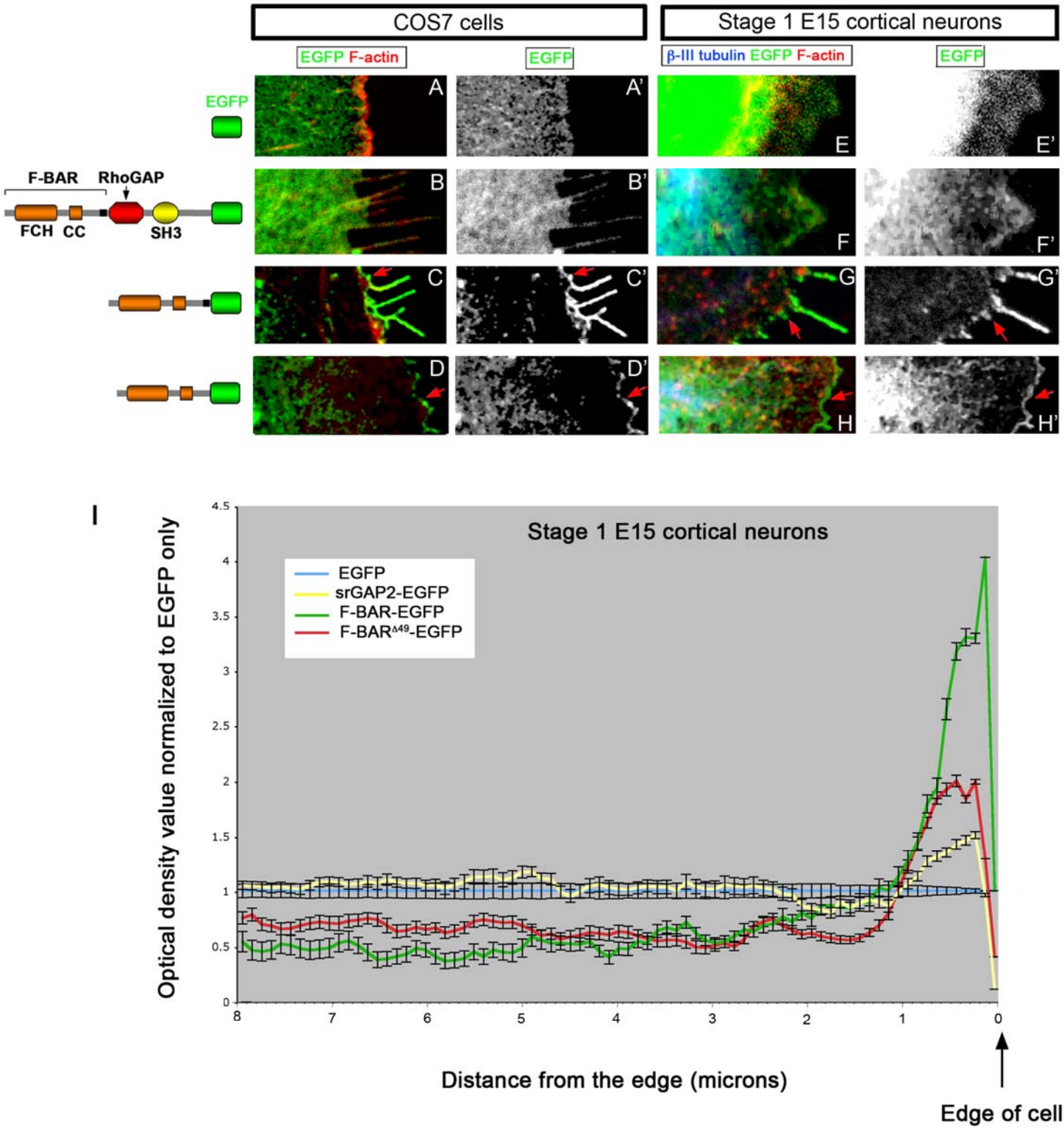

Figure S4. Quantification of the location of srGAP2-EGFP, F-BAR-EGFP and F-BAR$^{\Delta 49}$-EGFP fusion proteins in COS7 cells (**A-D'**) and Stage 1 E15 cortical neurons (**E-H'**; see text for detail). Note that in both cell types, the F-BAR-EGFP and the F-BAR$^{\Delta 49}$-EGFP are enriched at the plasma membrane (red

arrows). (**I**) Histogram of the optical density of EGFP signal for the four constructs examined as a function of distance from the edge of Stage 1 cortical neurons. The optical density for each EGFP fusion protein is normalized to the signal obtained for EGFP only, in order to normalize for variation of cytoplasmic volume.

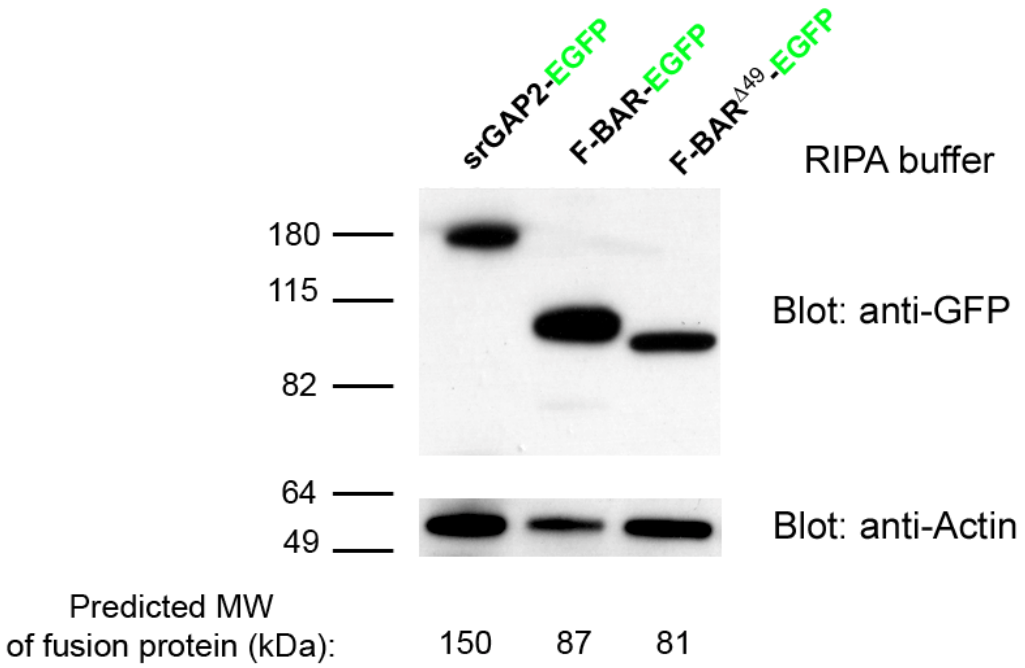

Figure S5. Proper expression of srGAP2-EGFP, F-BAR-EGFP and F-BAR$^{\Delta 49}$-EGFP fusion proteins in COS7 cells. COS7 cells were transfected with the indicated constructs and lyzed at 48h after transfection following a dual lysis procedure: co-immunoprecipitation buffer was made up of 50mM Tris-Cl (pH 7.4), 15mM EGTA, 100mM NaCl, 0.1% Triton-X, and then protease inhibitor, DTT (1mM), and PMSF (1mM). The insoluble portion of that (including the triton-insoluble protein fraction associated with membrane) was then subjected to a modified RIPA buffer: 50 mM Tris pH 7.4, 0.5% Na Deoxycholate, 0.2% SDS, 1 mM EDTA, 150mM NaCl, plus PMSF (1mM) and protease inhibitors. Proteins from the modified RIPA buffer soluble fraction were then separated by SDS-PAGE and blots were probed with anti-EGFP antibody (upper blot) or anti-actin antibody (lower blot). Note that each of these three constructs are expressed as a band at the expected molecular weight (indicated below the actin blot) although on this type of pre-casted gradient gels, proteins tend to migrate at a higher apparent MW.

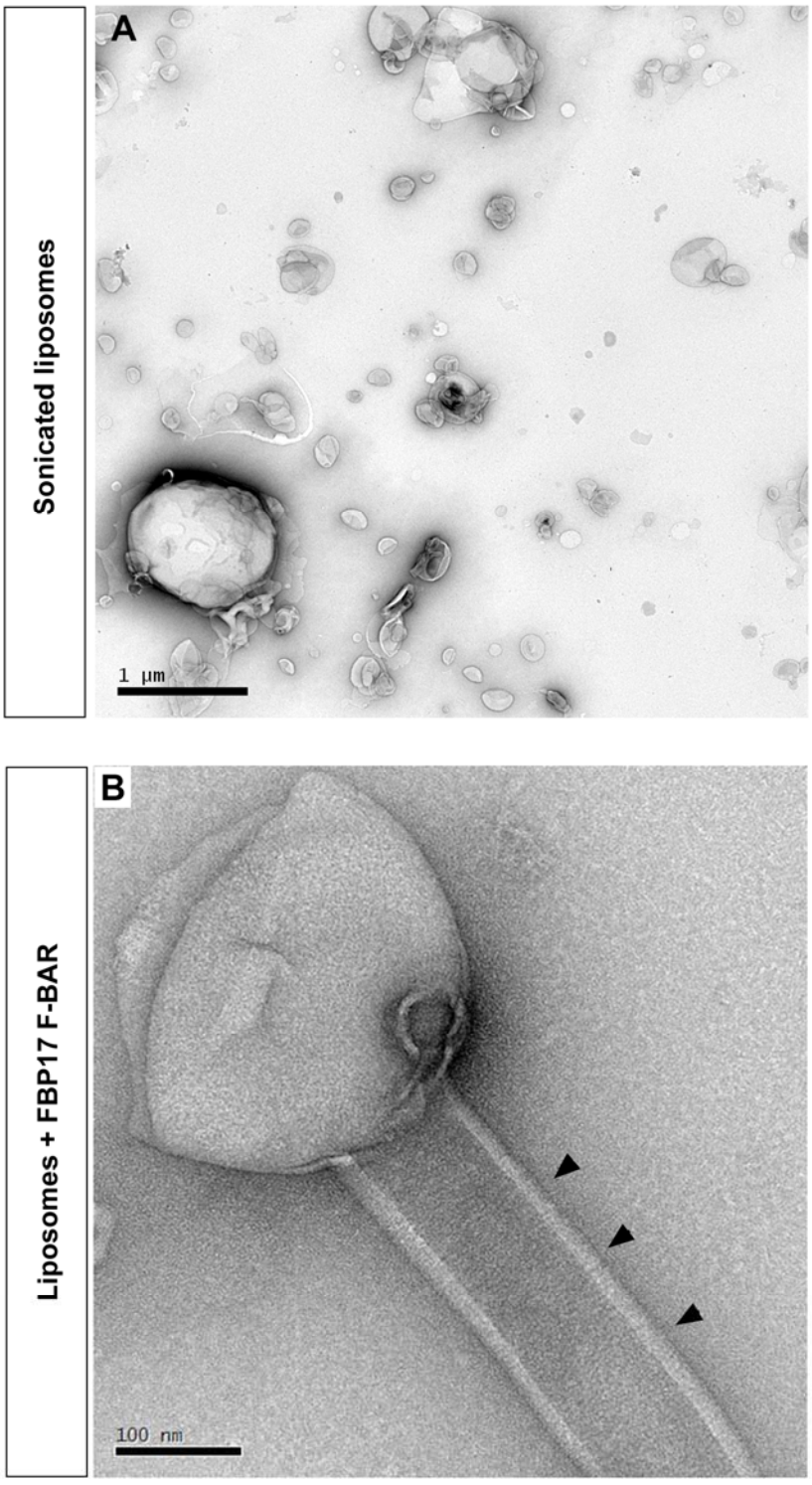

Figure S6. Control FBP17 F-BAR tubulates liposome.

(A) Normal morphology of control liposomes following sonication but without incubation with any recombinant protein. (B) The recombinant purified F-BAR domain of FBP17 incubated with preformed liposomes induces long tubulation (arrowheads).

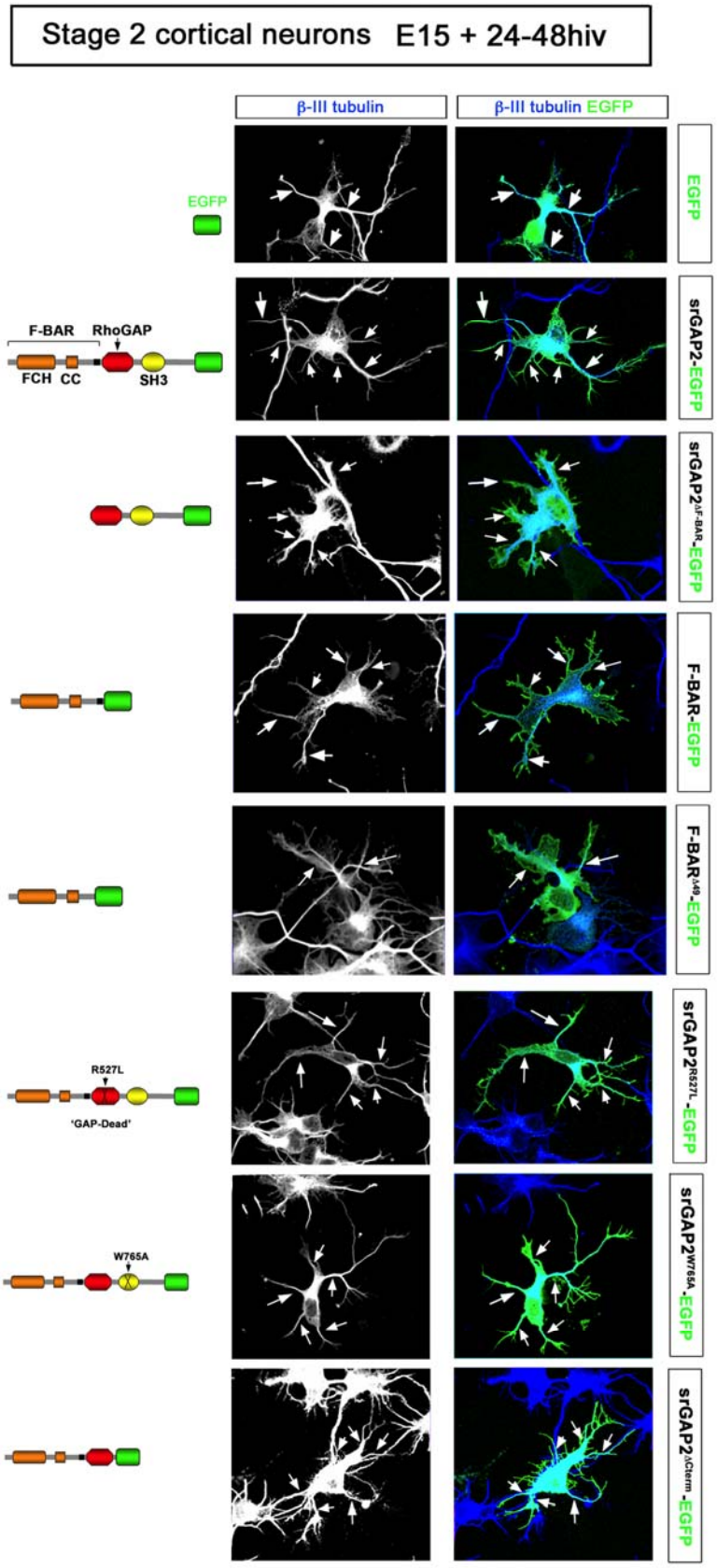

Figure S7. Neurites induced by different srGAP2 constructs contain microtubules. Compilation of all the images shown for Stage 2 E15 cortical neurons in Figure 4 and Suppl. Figure 12 showing the βIII tubulin signal (left panel) and the corresponding merged image with EGFP. The arrows indicate the presence of microtubules in all the neurites that were counted as 'primary' neurites emerging from the cell body.

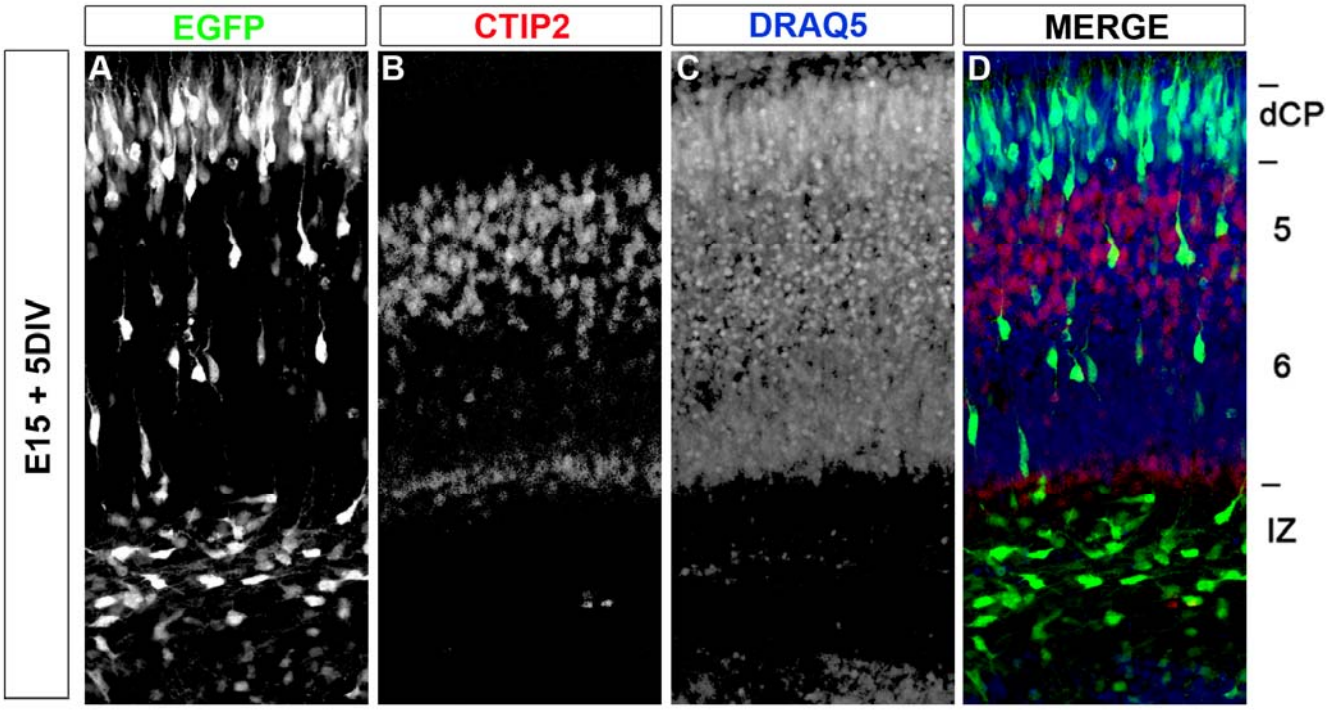

Figure S8. Definition of layers in slices following dorsal electroporation and organotypic culture.

(A-D) E15 cortical slices cultured for 5 days after electroporation with EGFP were fixed and stained with CTIP2 (layer 5/6 marker) as well as Draq 5 in order to reveal the cytoarchitecture. We use this laminar definition throughout the paper: dense Cortical Plate (dCP) defined as the densely packed, most immature neurons that migrated to the top of the cortical plate below the cell sparse marginal zone (MZ) and above CTIP2+ layer 5 neurons. The intermediate zone is defined by the low packing density visualized by Draq5 located under layer 5/6 and which contains neurons initiating radial migration.

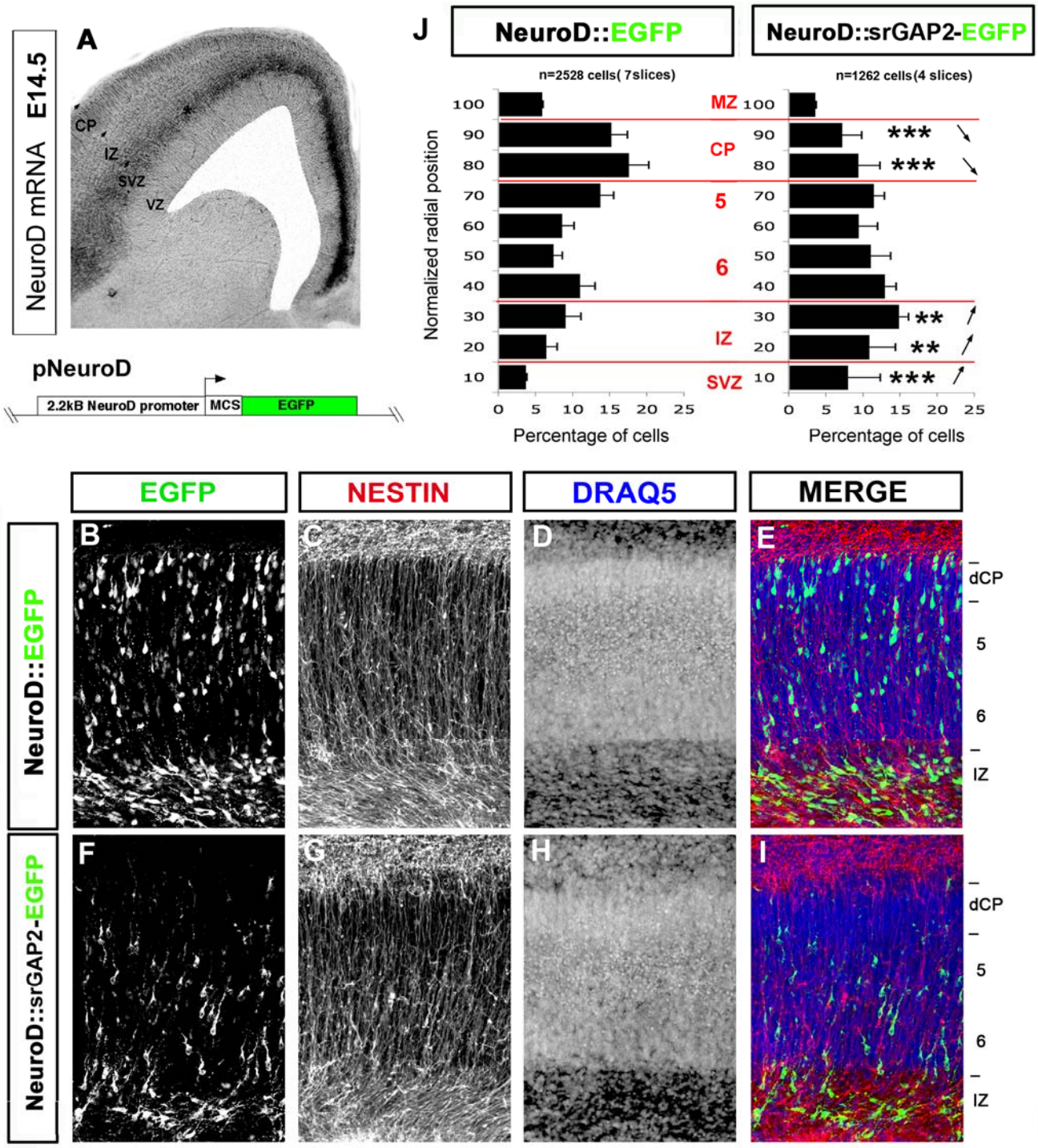

Figure S9. Expression of srGAP2 in post mitotic neurons inhibits radial migration.

(A) In situ hybridization of NeuroD mRNA in the developing neocortex of an E15 mouse embryo. *NeuroD* is expressed at the SVZ/IZ border but not in the VZ. Schematic representation of the construct used to express EGFP-fusion proteins under the control of the 2.2kB promoter region of NeuroD, which drives cDNA expression exclusively in post-mitotic neurons.

(B-I) E15 cortical slice cultured for 5 days after transfection with pNeuroD-EGFP or pNeuroD-srGAP2-EGFP. EGFP expressing neurons migrate nicely to the cortical plate (B-E). In contrast, srGAP2-EGFP expressing neurons migrate poorly to the cortical plate (F-I). Slices were stained with anti-nestin to reveal the radial glial scaffold and Draq5 to illustrate the cytoarchitecture.

(J) Quantification of B-G showing that a greater proportion of neurons reach the cortical plate in control (EGFP transfected) conditions than in srGAP2 transfected neurons (note decrease proportion of cells in CP and increase proportion in IZ (denoted by arrows) when compared to control). (EGFP n= 7 slices and srGAP2 n= 5 slice).

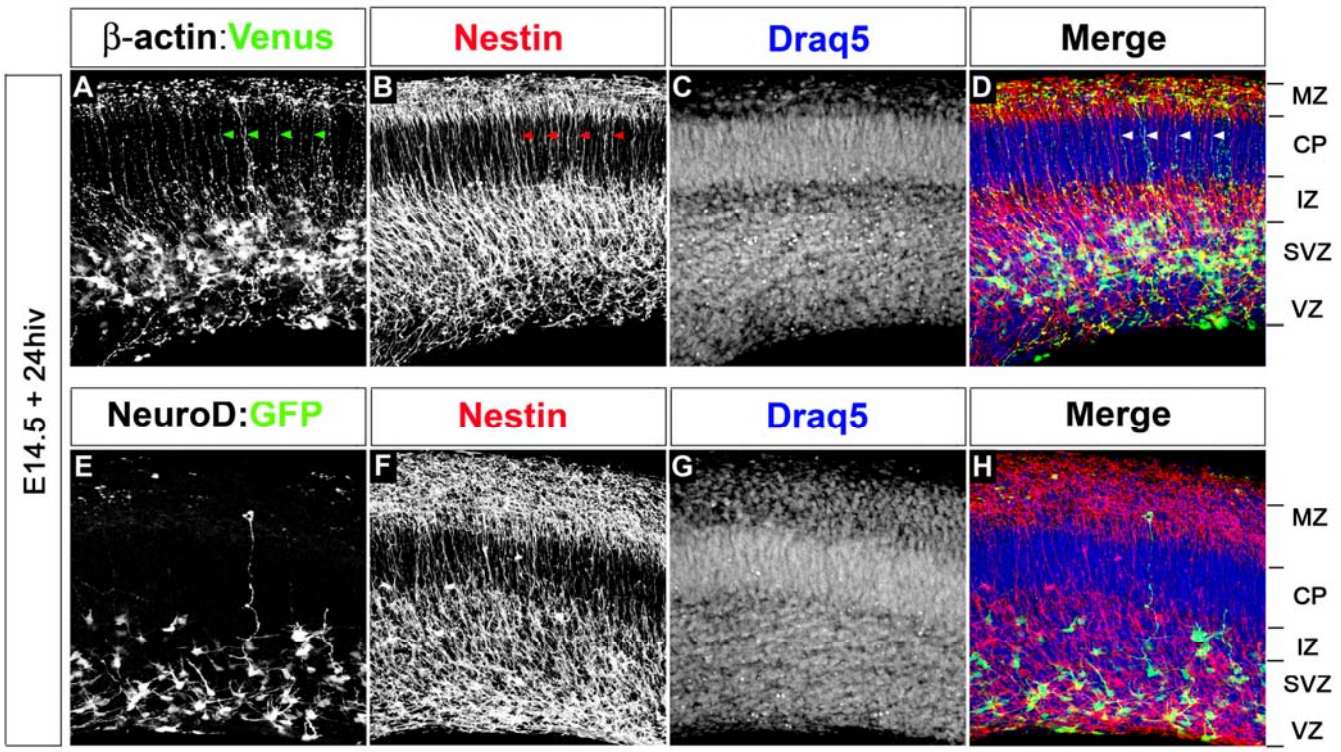

Figure S10. 2.2kD NeuroD promoter drives gene expression in non-radial glial intermediate progenitors 24 hours after electroporation.

(A-D) E15 cortices were electroporated chicken-β-actin driven Venus construct sliced and cultured for 24 hrs. After 24 hrs venus positive cells were also positive for anti-nestin (radial glia marker, green arrow heads in A, red arrowheads in B and white arrow heads in D). Also note the long radial glial like morphology of cells.

(F-H) In contrast NeuroD drive EGFP expression in non-radial glial intermediate progenitors that are Nestin-negative, supporting the idea that the NeuroD promoter drives expression in intermediate progenitors and early postmitotic neurons in the SVZ/IZ but not in radial glial progenitors in the VZ.

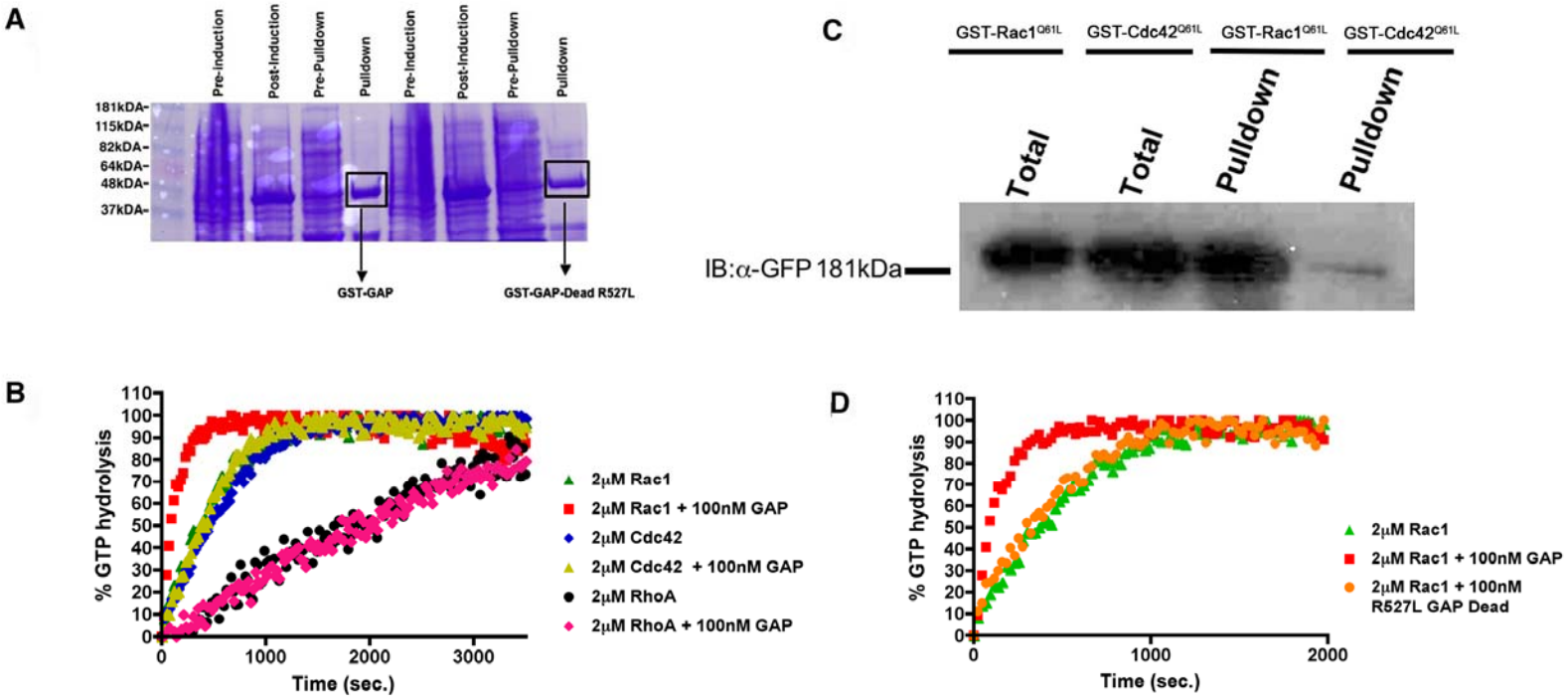

Figure S11. The RhoGAP domain of srGAP2 is specific for Rac1.

(A) GST-purification of the wild-type GAP and GAP^{R527L} forms of the RhoGAP domain of srGAP2. Coumassie-stained gel showing the yield recombinant proteins obtained before and after induction (lanes 1-2 and 5-6) in bacteria as well as before and after glutathione-elution of GST-GAP (lanes 3-4) and GST-GAP^{R527L} (lanes 7-8). The boxed areas correspond to the purified recombinant proteins used for the subsequent GTP hydrolysis assays in panel B-C.

(B) Fluorescent-based GTP hydrolysis assay as a function of time (seconds) for 2μM purified Rac1, Cdc42, RhoA in the presence or absence of 100nM of the recombinant GAP-domain of srGAP2. Note that the GAP domain of srGAP2 only accelerates the rate of GTP hydrolysis of Rac1 but not Cdc42 or RhoA.

(C) Same as B expect that 2μM purified Rac1 is incubated alone or in the presence of 100nM of recombinant wild-type GAP domain or GAP^{R527L}. Note that this point mutation abolishes the accelerating effect of the GAP domain on Rac1 GTP hydrolysis.

(D) GST pulldown of srGAP2-EGFP from COS7 cells using constitutively active forms of Rac1 (Rac1^{Q61L}) or Cdc42 (Cdc42^{Q61L}). GST-Rac^{Q61L} pulls down significantly higher amounts of srGAP2 compared to GST-Cdc42^{Q61L} confirming that this is a Rac1-specific GAP.

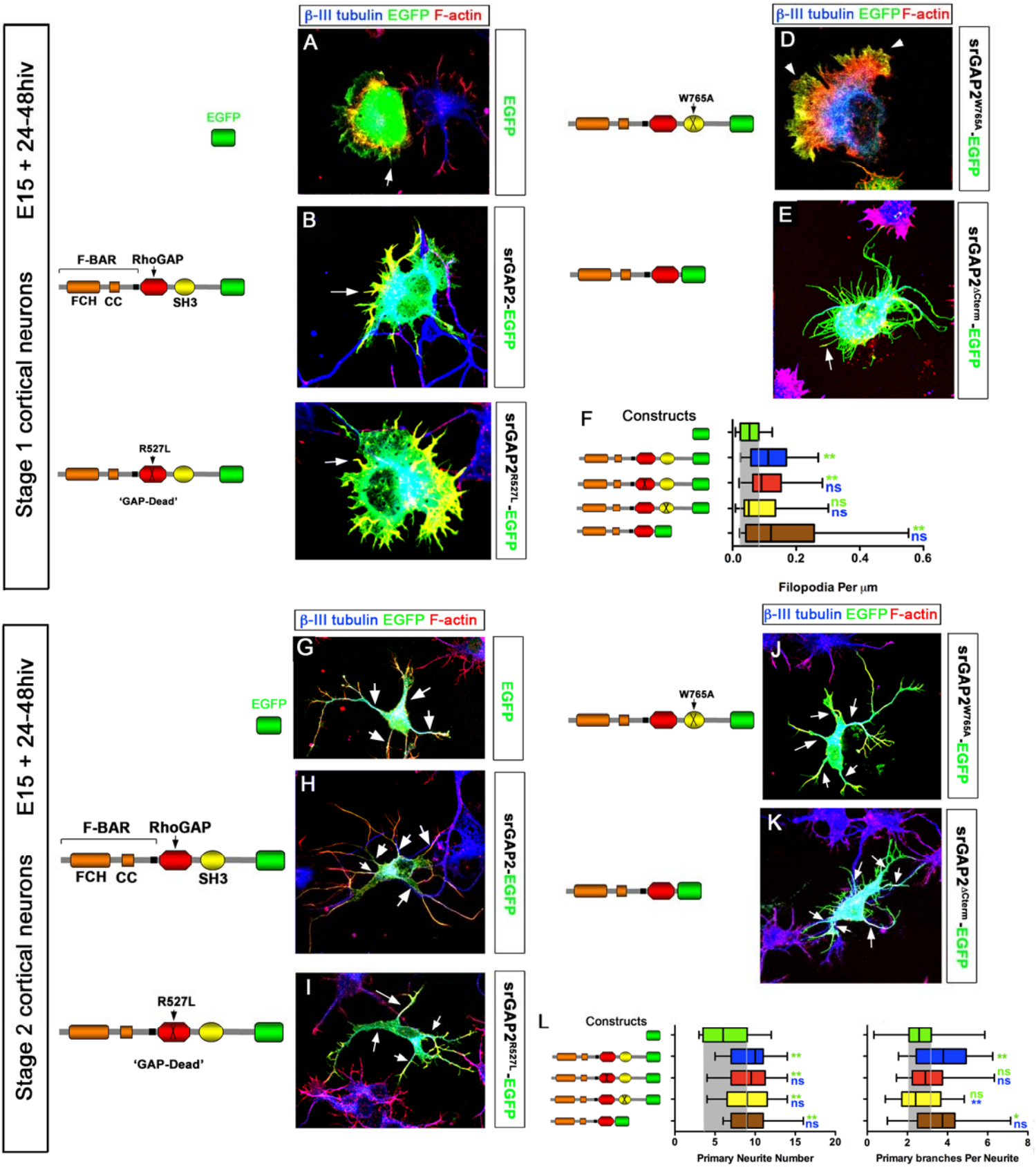
Stage 1 cortical neurons E15 + 24-48hiv
β-III tubulin EGFP F-actin
A
EGFP
EGFP
B
srGAP2-EGFP
F-BAR
RhoGAP
FCH CC
SH3
R527L
'GAP-Dead'
srGAP2R527L-EGFP
D
srGAP2W765A-EGFP
W765A
E
srGAP2ΔCterm-EGFP
F
Constructs
**
**
ns
ns
ns
**
ns
0.0
0.2
0.4
0.6
Filopodia Per μm
Stage 2 cortical neurons E15 + 24-48hiv
β-III tubulin EGFP F-actin
G
EGFP
H
srGAP2-EGFP
F-BAR
RhoGAP
FCH CC
SH3
R527L
'GAP-Dead'
I
srGAP2R527L-EGFP
J
srGAP2W765A-EGFP
W765A
K
srGAP2ΔCterm-EGFP
L
Constructs
**
**
ns
**
ns
**
ns
0
5
10
15
20
Primary Neurite Number
**
ns
ns
ns
**
*
ns
0
2
4
6
8
Primary branches Per Neurite

Figure S12. The GAP and SH3 domains participate in srGAP2's ability to promote filopodia formation in neurons.

(A-E) Stage 1 cortical neurons expressing various srGAP2 constructs. All cells are stained with β-III tubulin to indicate that it is a neuron and phalloidin to visualize F-actin.

Control stage 1 neurons (EGFP (A)) normally display filopodia at cell periphery. However expression of srGAP2-EGFP (B) significantly increased the number of filopodia. Mutation of the GAP domain (srGAP2^{R527L}-EGFP (B)) did not appear to affect the ability of srGAP2 to make filopodia but did appear to increase lamellapodia formation. The SH3 domain mutant (srGAP2^{W765A}-EGFP (D)) completely abrogated srGAPs ability to induce filopodia formation while deletion of the c-terminus (E) (including the SH3 domain, srGAP2$^{\Delta Cterm}$-EGFP) was able to induce filopodia.

(F) Quantification of A-E. (EGFP n= 20 cells; srGAP2-EGFP n= 21 cells; srGAP2^{R527L}-EGFP n= 21 cells; srGAP2^{W765A}-EGFP n= 21 cells; srGAP2$^{\Delta Cterm}$-EGFP n=20 cells. Cells were taken from 3 different experiments and analyzed using Mann-Whitney Test * $p<0.05$; ** $p<.001$; *** $p<0.001$. Green color indicates comparison to EGFP and blue color indicates comparison to srGAP2-EGFP)

(G-K) Stage 2 cortical neurons expressing various srGAP2 constructs. All cells are stained with β-III tubulin to indicate that it is a neuron and phalloidin to visualize F-actin.

As shown previously expression of srGAP2 (H) caused increase neurites initiation and branching compared to EGFP (G) expressing neurons at stage 2. Expression of srGAP2^{R527L}-EGFP (I); srGAP2^{W765A}-EGFP (J); and srGAP2$^{\Delta Cterm}$-EGFP (K) all caused increased neurite initiation. While, srGAP2$^{\Delta Cterm}$-EGFP expression caused significant increases in neurite branching (K), srGAP2^{W765A}-EGFP expression (I) had no effect. Expression of srGAP2^{R527L}-EGFP did cause an increase in neurite branching, but not as significant as srGAP2.

(L) Quantification of G-K. (EGFP n= 20 cells; srGAP2-EGFP n= 21 cells; srGAP2^{R527L}-EGFP n= 22 cells; srGAP2^{W765A}-EGFP n= 21 cells; srGAP2$^{\Delta Cterm}$-EGFP n=23 cells. Cells were taken from 3 independent experiments and analyzed using Mann-Whitney Test * $p<0.05$; ** $p<.001$; *** $p<0.001$).

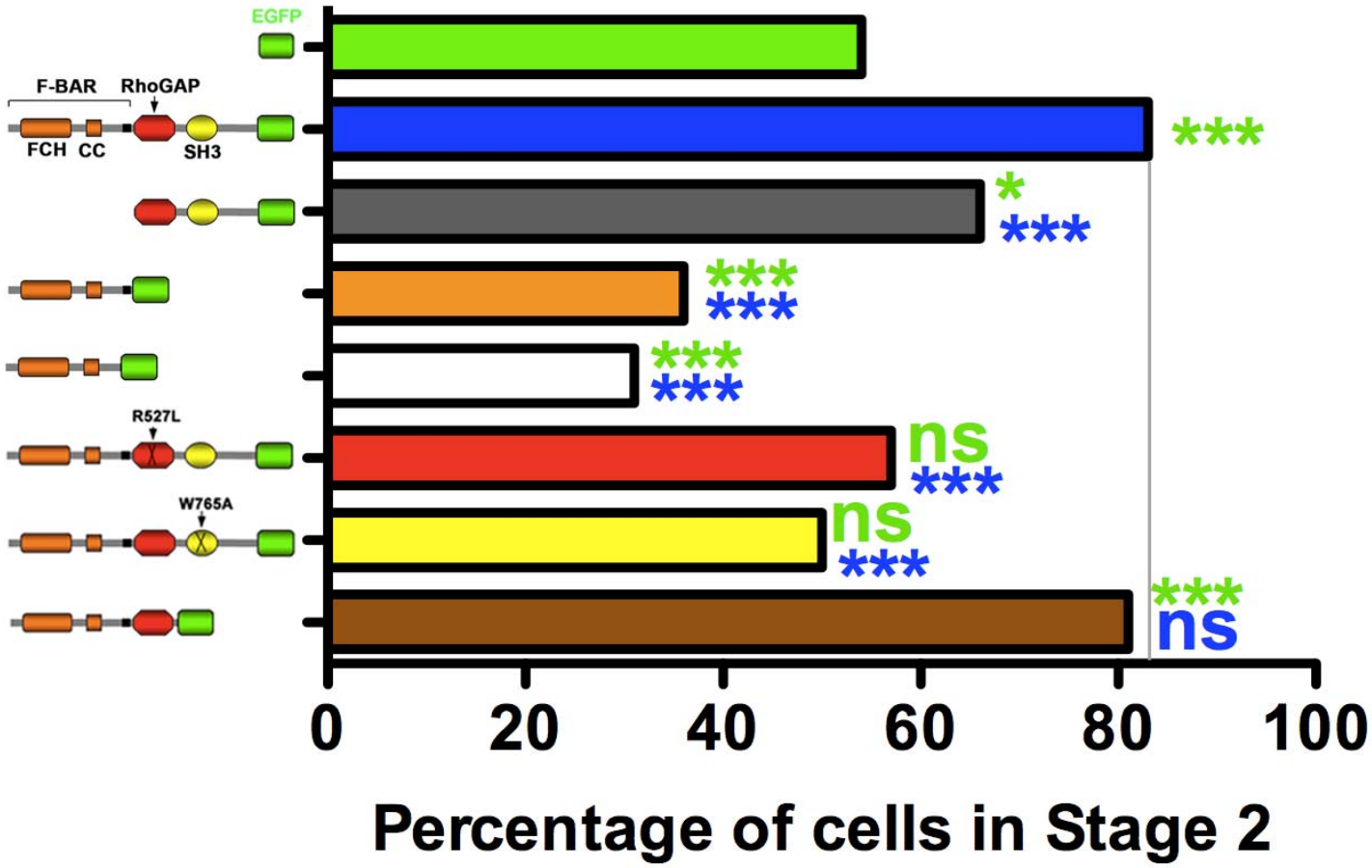

Figure S13. srGAP2 expressing cells accumulate in Stage 2

Analysis of the percentage of cells that accumulate at Stage 2 after transfection of various srGAP2 constructs. (n>80 neurons in each conditions).

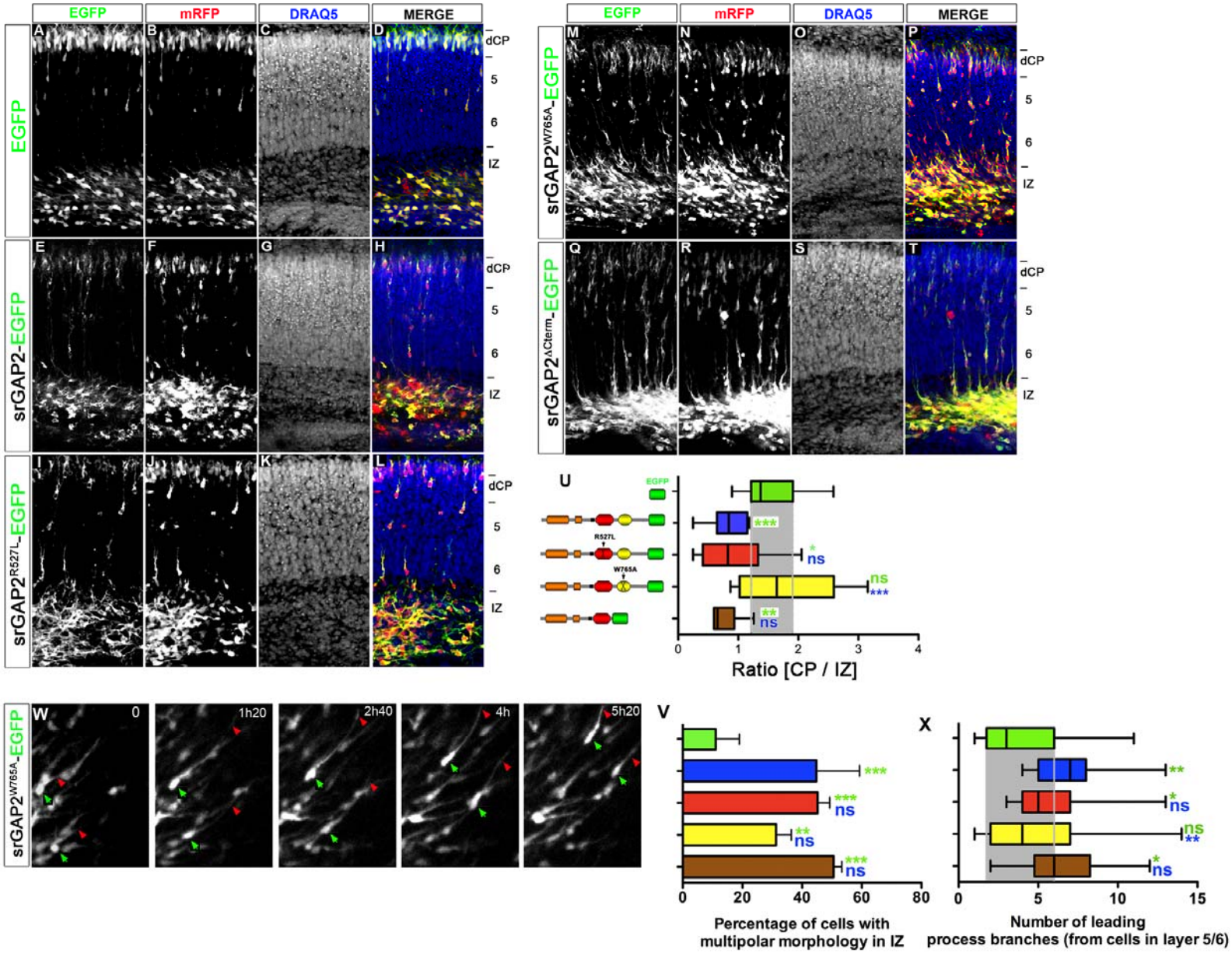

Figure S14. The GAP and SH3 domains participate in srGAP2's ability to inhibit migration.

(A-T) E15 cortical slices cultured for 5 days after electroporation with various srGAP2 constructs and mRFP. Slices were stained with Draq5 in order to demonstrate cytoarchitecture. As shown previously srGAP2 expressing neurons migrate very poorly to the cortical plate (E-H)

Impairment of the GAP activity of srGAP2 (srGAP2^{R527L}) inhibits migration albeit not to the degree of full-length srGAP2 (I-L). Moreover, mutation of the SH3 domain (srGAP2^{W765A}) (M-P) had no effect on the ability of neurons to migrate, in that it does not inhibit migration like full-length srGAP2. However, expression of the c-terminal deletion of srGAP2 (srGAP2$^{\Delta Cterm}$-EGFP) does impair migration (Q-T).

(U) Quantification of effects displayed in A-L. (EGFP, n= 13 slices; srGAP2-EGFP n= 14 slices; srGAP2^{R527L}-EGFP n= 11 slices; srGAP2^{W765A}-EGFP n= 8 slices; srGAP2$^{\Delta Cterm}$-EGFP n= 6 slices.

Slices were taken from 4 independent experiments and analyzed using Mann-Whitney Test * $p<0.05$; ** $p<.001$; *** $p<0.001$. Green color indicates comparison to EGFP and blue color indicates comparison to srGAP2-EGFP).

(V) Quantification of percentage of cells with multipolar morphology in EGFP, srGAP2, or F-BAR transfected slices. Multipolar cells were defined as cells possessing $\geq$ 3 processes. (EGFP n= 66 cells; srGAP2-EGFP n= 42 cells; srGAP2^{R527L}-EGFP n= 47 cells; srGAP2^{W765A}-EGFP n= 52 cells; srGAP2$^{\Delta Cterm}$-EGFP n= 50 cells. Cells were taken from 3 independent experiments and analyzed using Mann-Whitney Test * $p<0.05$; ** $p<.001$; *** $p<0.001$. Green color indicates comparison to EGFP and blue color indicates comparison to srGAP2-EGFP).

(W) Time-series of E15 cortical slices cultured for 3 days after electroporation with srGAP2^{W765A}-EGFP (coelectroporated with venus plasmid). These neurons showed a unipolar morphology with a single unbranched leading process (red arrowhead) and translocated very efficiently (green arrowhead).

(X) Quantification of leading process branching from cells expressing EGFP, srGAP2-EGFP, srGAP2^{R527L}-EGFP, srGAP2^{W765A}-EGFP, or srGAP2$^{\Delta Cterm}$-EGFP in layer 5/6. (EGFP n= 17 cells; srGAP2-EGFP n= 21 cells; srGAP2^{R527L}-EGFP n= 18 cells; srGAP2^{W765A}-EGFP n= 26 cells; srGAP2$^{\Delta Cterm}$-EGFP n= 18 cells. Cells were taken from 3 independent experiments and analyzed using Mann-Whitney Test * $p<0.05$; ** $p<.001$; *** $p<0.001$. Green color indicates comparison to EGFP and blue color indicates comparison to srGAP2-EGFP).

SUPPLEMENTAL REFERENCES

Edgar, R.C. (2004). MUSCLE: multiple sequence alignment with high accuracy and high throughput. Nucleic Acids Res *32*, 1792-1797.

Hand, R., Bortone, D., Mattar, P., Nguyen, L., Heng, J.I., Guerrier, S., Boutt, E., Peters, E., Barnes, A.P., Parras, C.*, et al.* (2005). Phosphorylation of Neurogenin2 specifies the migration properties and the dendritic morphology of pyramidal neurons in the neocortex. Neuron *48*, 45-62.

Mattar, P., Britz, O., Johannes, C., Nieto, M., Ma, L., Rebeyka, A., Klenin, N., Polleux, F., Guillemot, F., and Schuurmans, C. (2004). A screen for downstream effectors of Neurogenin2 in the embryonic neocortex. Dev Biol *273*, 373-389.

Pei, J., Kim, B.H., and Grishin, N.V. (2008). PROMALS3D: a tool for multiple protein sequence and structure alignments. Nucleic Acids Res *36*, 2295-2300.

Polleux, F., and Ghosh, A. (2002). The slice overlay assay: a versatile tool to study the influence of extracellular signals on neuronal development. Sci STKE *2002*, PL9.

Soding, J., Biegert, A., and Lupas, A.N. (2005). The HHpred interactive server for protein homology detection and structure prediction. Nucleic Acids Res *33*, W244-248.

Yao, Q., Jin, W.L., Wang, Y., and Ju, G. (2008). Regulated shuttling of Slit-Robo-GTPase activating proteins between nucleus and cytoplasm during brain development. Cell Mol Neurobiol *28*, 205-221.